CrossMark

ORIGINAL ARTICLE

Automatic measurement and visualization of focal femoral cartilage thickness in stress-based regions of interest using three-dimensional knee models

Marios Pitikakis[1] · **Andra Chincisan[2]** · **Nadia Magnenat-Thalmann[2]** ·
Lorenzo Cesario[1] · **Patrizia Parascandolo[1]** · **Loris Vosilla[1]** · **Gianni Viano[1]**

Abstract

Purpose Thinning of cartilage is a common manifestation of osteoarthritis. This study addresses the need of measuring the focal femoral cartilage thickness at the weight- bearing regions of the knee by developing a reproducible and automatic method from MR images.

Methods 3D models derived from semiautomatic MR image segmentations were used in this study. Two different methods were examined for identifying the mechanical loading of the knee articulation. The first was based on a generic weight-bearing regions definition, derived from gait characteristics and cadaver studies. The second used a physically based simulation to identify the patient-specific stress distribution of the femoral cartilage, taking into account the forces and movements of the knee. For this purpose, four different scenarios were defined in our 3D finite element (FE) simulations. The radial method was used to calculate the cartilage thickness in stress-based regions of interest, and a study was performed to validate the accuracy and suitability of the radial thickness measurements.

Results Detailed focal maps using our simulation data and regional measurements of cartilage thickness are given. We present the outcome of the different simulation scenarios and discuss how the internal/external rotations of the knee alter the overall stress distribution and affect the shape and size of the calculated weight-bearing areas. The use of FE simulations allows for a patient-specific calculation of the focal cartilage thickness.

Conclusion It is important to assess the quantification of focal knee cartilage morphology to monitor the progression of joint diseases or related treatments. When this assessment is based on MR images, accurate and robust tools are required. In this paper, we presented a set of techniques and methodologies in order to accomplish this goal and move toward personalized medicine.

Keywords Cartilage thickness · Knee · MRI · 3D models · Weight-bearing areas · Stress simulation · Computer-aided diagnosis

✉ Marios Pitikakis
  marios.pitikakis@gmail.com

  Andra Chincisan
  andra.chincisan@miralab.ch

  Nadia Magnenat-Thalmann
  thalmann@miralab.ch

  Lorenzo Cesario
  lorenzo.cesario@softeco.it

  Patrizia Parascandolo
  patrizia.parascandolo@softeco.it

  Loris Vosilla
  loris.vosilla@softeco.it

  Gianni Viano
  gianni.viano@softeco.it

[1] Sosteco Sismat S.r.l., Genoa, Italy

[2] MIRALab, University of Geneva, Geneva, Switzerland

Introduction

Accurate and precise assessments of cartilage thickness are important for addressing a number of clinical questions for the prevention, treatment and progression of osteoarthritis (OA), which is a major and increasing public health problem [1]. Knee OA is characterized mainly by the progressive erosion and loss of articular cartilage. Recent analyses suggest cartilage loss in OA to be in the range of 0.5–2.0 % per year [2]. Cartilage thickness and volume measurements are morphological biomarkers for OA that can be assessed from MR images [3].

🌀 Springer

Early work used three-dimensional (3D) fat-suppressed spoiled gradient-echo sequences, followed by manual slice-by-slice segmentation of cartilage and measurements of global volume or mean thickness [4,5]. These global measurements are too generic, and, in order to detect the heterogeneous nature of cartilage loss during OA disease progression, a more refined analysis is needed to enable measurements of focal anatomical regions.

The mechanical loading during walking has been shown to influence the progression of osteoarthritis at the knee as well as the outcome of treatment, while accurate and precise assessments of in vivo femoral cartilage thickness are essential for addressing a number of clinical research questions. [6]. However, OA is not a purely biomechanical disease. The complexity of the knee joint and the fact that it is an active weight-bearing joint are factors in making the knee one of the most commonly injured joints. An injury can change the normal patterns of loading or affect the cartilage, ligaments, menisci, etc., and OA can also be manifested in nonstress-related areas.

Several studies have demonstrated that the loss of cartilage in patients with knee OA is generally progressive over time [7,8]. Pelletier et al. [9] confirmed that joint space width (JSW) narrowing is strongly associated with femoral cartilage loss in weight-bearing areas. Other researchers use regional measurements of cartilage thickness to provide focal information [10] and statistical models of the bones' appearance and shape were used to construct detailed maps showing changes in cartilage thickness over time [11]. Others automate the task of identifying anatomical regions by dividing the cartilage based on the geometry of its outer edges [12]. Tamez-Peña et al. [13] automatically divided the femoral cartilage into five anatomical regions. Duryea et al. [14] focused on location-specific JWS and developed a semiautomatic method for local area cartilage segmentation and measurement of cartilage loss.

Although these methods account for shape and scale variations, either global or local, they do not account for precise region boundaries that can vary between patients. The separation of weight bearing from the nonweight-bearing regions of the knee joint is an important condition. Obtaining accurate measurements, however, is a challenging task, partly because knee cartilage is very thin and has complex curvy shapes. Previous studies demonstrated that biomechanical model simulations of the knee articulation can provide useful insight in the evolution of the osteoarthritis in the knee cartilage [15,16]. The finite element (FE) method has been a popular solution for the simulation of deformable elastic solids. In the last two decades, different anatomical models have been proposed in the literature to model the human tissues using the FE method [17,18].

In this paper, we present and evaluate an automated method for calculating the subject-specific cartilage thickness at the weight-bearing areas for the distal femur, based on the bone geometry of 3D models derived from MR images. First, an overview of our algorithm is given. Afterward, we define and calculate the focal cartilage thickness in two different ways: by using generic weight-bearing regions based on normal gait characteristics and cadaver studies, and by using a physically based simulation to identify the patient-specific stress distribution of the femoral cartilage, taking into account the forces and movements of the knee articulation. To our knowledge, this is the first paper that uses 3D finite element (FE) simulations of subject-specific models and calculates the focal cartilage thickness. Finally, we compare and summarize our simulation results, evaluate the radial thickness measurements and conclude our work with some notable observations and a discussion.

Materials and methods

Image acquisition

Five healthy male volunteers were included in the study. Each subject had the same knee examined in a resting supine position using a hybrid PET-MR 3.0T scanner (Philips Ingenuity TF PET/MRI). Ethical approval for the study was obtained from the Ethical Committee for Research on Humans (CEREH) of the Geneva University Hospitals and the Swiss Agency for Therapeutic Products. All the volunteers signed an informed consent form (Table 1).

Images were obtained using a 3D isotropic sequence VISTA SPAIR (volume isotropic turbo spin echo acquisition). In total, 458 slices were acquired with a voxel size of $0.33 \times 0.33 \times 0.35 \, mm^3$.
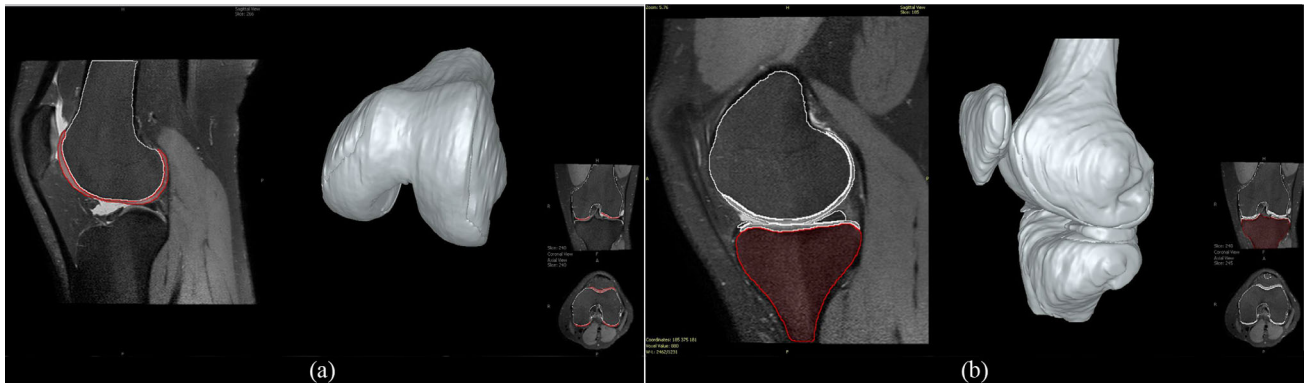
Segmentation and 3D model reconstruction

In this study, we applied an interactive segmentation approach that combines the efficiency, accuracy and repeatability of automatic segmentation methods with the expertise and quality assurance that can derive from human supervision. We used RheumaSCORE [19,20], a computer-aided diagnosis (CAD) software application developed by Softeco Sismat S.r.l. [21] that supports and assists the user during the diagnosis and the management of chronic diseases such as rheumatoid arthritis (RA) [22,23] through the processing, analysis, display, measurement and the comparison of MRIs. RheumaSCORE's segmentation features are based on an interactive real-time level-set algorithm introduced in [24]. Level-set algorithms have already proved their potential [25,26] and have been increasingly applied for 3D medical image segmentation.

The segmentations were performed by a single user and reviewed by two more experienced users. Femur, tibia and

Table 1 Details of volunteer subjects relevant to the study

Subject	Age (y)	Height (m)	Mass (kg)	Body mass index (kg/m^2)
1	26	1.75	85	27.8
2	25	1.72	62	21.0
3	29	1.97	84	21.6
4	22	1.76	68	22.0
5	32	1.73	58	19.4

Fig. 1 Subject 1 MRI and segmentation of the femoral cartilage (**a**), tibia (**b**) and 3D model reconstruction of all knee elements

patella bones, cartilages and menisci elements were segmented using a semiautomatic approach. Initially, a geodesic level-set algorithm was applied to every element. The segmentation was interactive and user driven, i.e., the algorithm evolution was influenced by changing the default speed function parameters and iteratively converged to the desired result. Our method does not require prior identification of the bones (femur and tibia) for the segmentation of the articular cartilages within the knee. However, the software supports the automatic definition of regions of interest (ROI) for more accurate and faster cartilage segmentation, if the bones are already segmented. After this step, some manual corrections were performed to refine the segmented images.

The anatomical structures of the subject-specific models were reconstructed using surface rendering (marching cubes algorithm [27]). Figure 1 highlights the corresponding femoral cartilage segmentation, tibia segmentation and the generated 3D reconstructions of our first volunteer subject.

Cartilage thickness algorithm overview

For our cartilage thickness measurements, we mainly utilize the triangle mesh models (in VTK format) of the femur and femoral cartilage. The mesh model of the tibia is used only for visual confirmation purposes. Our methodology for calculating the thickness of the femoral cartilage consists of the following steps:

(a) *Calculate the center of the rays for each condyle.* We use the overall femoral cartilage geometry to perform a direct cylindrical fitting. Then, we calculate the central axis and radius of the circular cylinder mesh. An additional step was used to compensate for any rotation of the knee caused, e.g., by the acquisition method, the position of the subject or the device: The cylindrical axis was aligned to the *x*-axis and, as a result, all mesh models were transformed accordingly. This way the weight-bearing region definitions are independent of these rotations. Finally, the ray centers (located on the cylindrical axis and in the middle of each condyle) were identified. The ray centers are needed for the radial thickness calculations.

(b) *Define the weight-bearing region for each condyle.* For our study, we used two different methods of defining the weight-bearing regions. The first one is more generic and based on the approach proposed by Koo et al. [6], in which these regions are identified using normal gait characteristics and cadaver studies. The second method is more patient specific, using a physically based simulation to identify the stress distribution areas of the femoral cartilage. Details on both methods can be found in the following sections of this paper.

(c) *Radial thickness calculation.* The rays (directions) for the distance calculation were created only for the points that belong to the area of interest. Then, for every pair of inner and outer cartilage surface points with the same polar coordinates (i.e., the two intersections of the ray with the cartilage surface), we calculate the radial distance between them and generate a thickness map.
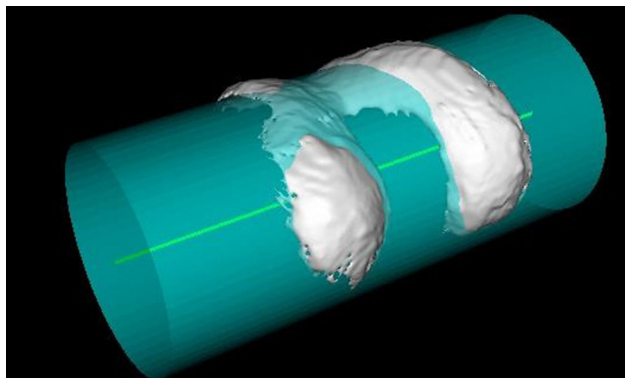
Cylindrical fitting

Surface fitting estimates the parameters of the surface primitives to represent the data. We focused on quadric surfaces, and specifically cylinders, because the geometry of the femoral inner boundary can be represented by a cylindrical coordinate system [28]. Quadric fitting is usually formulated as a nonlinear least-squares problem, which is solved either by using iterative methods for minimizing a nonlinear function or by directly solving the eigenvalue problem and no approximate values for the parameters are needed. Efficient quadric-fitting methods typically work in two steps. First, a linear direct method (typically an algebraic fitting method) generates an initial guess, and then, a nonlinear iterative method is used to refine that guess [29,30].

In our case, we chose direct fitting of a quadric surface to our triangle meshes with a specific quadric type: a circular cylinder. Without any constraints on the quadric type, even small amounts of noise can cause the result to have an undesired quadric type. For implementing our cylindrical fitting, we used the methods and libraries described in [31], i.e., solving the generalized eigenvalue problem with standard linear algebra packages (LAPACK [32]) and minimizing the nearly unbiased linear error metric introduced in [33] to ensure good results.

The direct cylindrical fitting was used for identifying the central axis perpendicular to the sagittal plane using the overall femoral cartilage geometry (see Fig. 2). For this particular study and since all of our subjects were healthy, we used the cartilage surface for the cylindrical fitting. However, we already implemented a variation in the algorithm that uses the bone geometry for the cylindrical fitting in case the cartilage surface is damaged or affected by OA.

Once the cylinder has been fitted to the cartilage, a local coordinate system (LCS) is defined. Each point can be located onto the corresponding surface by a simple coordinate transform. This way we can subdivide the weight-bearing areas on each condyle into anatomically defined subregions.
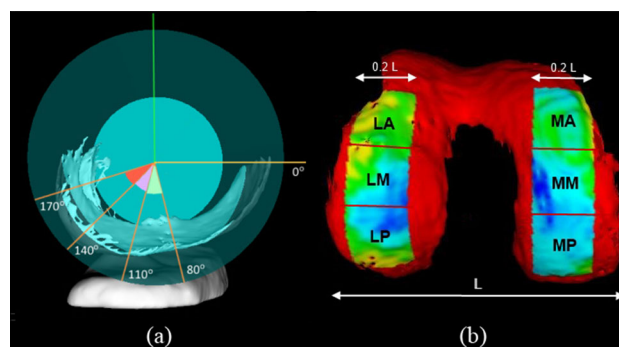
Identifying the weight-bearing regions

As mention earlier, our first method for identifying the weight-bearing regions of the cartilage that sustain contact during walking is based on normal gait characteristics of the knee flexion angles.

According to Koo et al. [6], which was based on cadaver studies, the tibiofemoral contact points were identified on each medial and lateral compartment. The contact point on the lateral condyle occurs at the most inferior point of the condyle, while the medial condyle contact point occurs about 20° anterior of the lateral condyle contact point. Six subregions of interest, three on each condyle, were identified on the cartilage. The width of the weight bearing region was estimated as 20 % of the overall maximal medial lateral cartilage width for each condyle.

In our study, the load-bearing areas are identified in a similar way as [6] and obtained as follows. The projection of the ray center along the y direction marks the 0°-axis of the cylindrical coordinate system on the femur. To avoid any dependence on the positioning of the knee or the orientation of the acquisition, an additional step was added, as mentioned earlier in the cartilage thickness algorithm overview. The alignment of the cylindrical axis with the x-axis, and the consequent alignment of all the meshes, ensures the reproducibility of the definition of the LCS and the marking of the 0°-axis.

The lateral condyle is then divided at 80°, 110°, 140° and 170°, i.e., 80° angle of offset, from the 0°-axis point toward the posterior aspect of the lateral condyle. Due to the fact that the medial condyle contact point occurs anterior of the lateral condyle contact point, the medial condyle is divided at 65°, 95°, 125° and 155° from the 0°-axis point toward the posterior aspect of the medial condyle, i.e., 65° angle of offset which is 15° anterior of lateral condyle (Fig. 3).

Fig. 2 Direct quadric (circular cylinder) fitting to the whole femoral cartilage surface mesh

Fig. 3 Six regions on the load-bearing areas are defined using our LCS, each of which correspond to a 30° rotation on the cylinder (**a**) and has a width equal to 20 % with the total width of the cartilage (**b**)
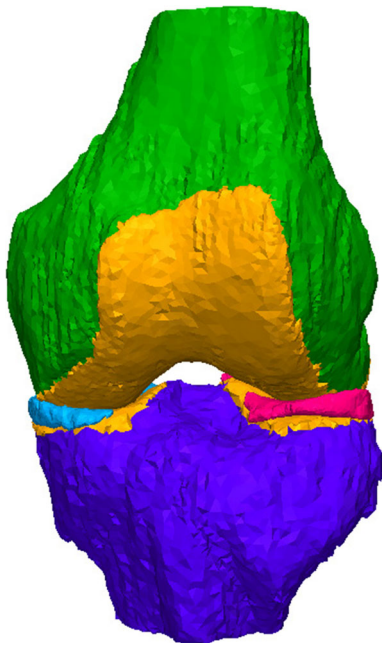
Fig. 4 3D knee articulation model of subject 1 used in the FE simulation

The above divisions define six distinct pieces of cartilage, three medial and three lateral, taking into account the three knee flexion angles during normal walking, typically at 0°, 30° and 60° based on the gait cycle. The width of each piece is defined at 20 % of the overall medial–lateral width of the femoral cartilage and centered around the centroid of each condyle. The centroid is calculated as the projection of the center of mass onto the central axis of the fitted cylinder.

The laterality, i.e., the distinction between the lateral and medial condyle, left or right knee, is calculated based on the volume of the condyle. The lateral condyle has a larger volume than the medial.

Finite element simulations for identifying the cartilage stress areas

We performed physically based simulations to investigate the tissue deformation and identify the effective stress distribution of the femoral cartilage.

The femur, tibia, menisci and articular cartilage structures were smoothed and then converted in volumetric meshes with tetrahedral elements (using CGAL [34]) in order to take advantage the simplicity and flexibility of the tetrahedral meshes (Fig. 4).

The material properties were modeled according to the values proposed by Sibole et al. [35] for the OpenKnee project. Due to their high stiffness with respect to the significant soft tissues, the bones were considered rigid bodies. The articular cartilage was defined as a nearly incompressible Mooney-Rivlin material, while the menisci were modeled as a Fung orthotropic hyperelastic material. The boundary conditions were modeled as follows: three contact frictionless surfaces were defined between the soft tissues of femoral cartilage–tibial cartilage, femoral cartilage–menisci and tibial cartilage–menisci.

During the compressive force, passive flexion and internal/external rotation simulations, the tibia was kept fixed in all six degrees of freedom, while the femur was allowed to move in these directions. The menisci were fixed on the tibial cartilage; however, the model allowed the deformation and the extrusion of the menisci. Only the points from the undersurface of the menisci were fixed on the tibia plateau. The femoral cartilage and tibial cartilage were attached to the bone surface. A rigid interface was defined between the bone and the corresponding cartilage. Hence, the selected nodes of the cartilage were constrained to move according to the rigid body. The femur axis origin was determined based on the best cylinder fit method. The cylinder's center represented the origin of the femoral anatomical coordinates and the center of rotation.

The nonlinear finite element (FE) solver FEBio [36] was used to perform the numerical simulations. Four different scenarios were investigated:

(i) 850 N axial compression force.
(ii) 100 N compression force and 45° passive flexion.
(iii) 10° external rotation.
(iv) 10° internal rotation.

The first scenario investigated an axial compression force of 850 N representing the body weight (BW) of the subject. The second scenario investigated the effect of passive flexion in the weight-bearing regions of the knee articulation. The last two scenarios modeled a 10° internal/external rotation. The selected movements (kinematics and forces) are within the physiological range of daily activities [37,38].

Cartilage thickness measurement

There are several definitions of thickness, e.g., closest thickness and normal thickness. However, for structures of volumetric layers with near-spherical morphology, the *radial thickness* is a more suitable thickness measurement [39].

Radial thickness determines the thickness of a volumetric layer as the distance between each pair of corresponding points on the two surfaces (or the inner and outer point of a single surface) with the same polar coordinates. An implementation of the fast ray/triangle intersection algorithm [40] was used to measure the thickness of the femoral cartilage, focused on the weight-bearing regions.

A study was performed to validate the accuracy and suitability of the radial method and to determine the variations in the calculation of the femoral cartilage thickness. To sim-
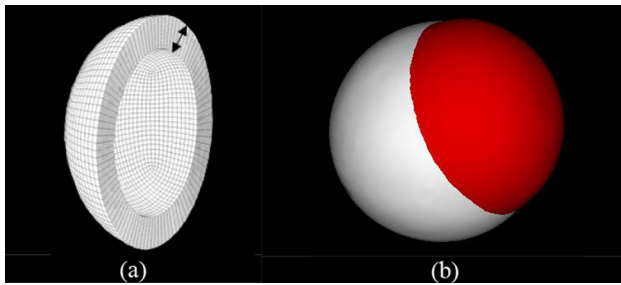
Fig. 5 Validating the accuracy of the radial thickness method using: **a** concentric spheres and **b** overlapping spheres creating a spherical cap

ulate the femoral cartilage, different mesh models of spheres were generated having known and predefined distance from each other. We used two test cases: (a) two spheres with the same center and known radius, and (b) two overlapping spheres with different centers, thus creating a spherical cap (see Fig. 5). To create the mesh models, DICOM images were generated with voxel dimensions $1 \times 1 \times 1$ mm and then segmented using a region-growing algorithm. The 3D models were generated with a marching cubes algorithm.

The cartilage thickness near the femoral condyles has mean values in the ranges of 1.65–2.65 mm and standard deviations 0.29 and 0.34, respectively [41]. Therefore, the master sphere in case (a) was created with a radius of 20 mm and the second sphere with a radius ranging from 20.5 to 23 with 0.5 mm increments (six test cases in total). Table 2 summarizes our quantitative results.

In case of (b), both spheres were created with a radius of 20 mm, but the second sphere had a small shift in its center in order to produce the cap. We chose to shift the center only along the x-axis just to simplify the calculations. The spherical cap has a variable thickness depending on the chosen point, with a minimum value around the points where the two spheres intersect and a maximum value along the x-axis equal to the shift of the second sphere center.

The radial thickness was computed both analytically (known real thickness) and with our algorithm. The sphere center shift used in our test cases was: (i) 2 mm, (ii) 3 mm, (iii) 4 mm and (iv) 5 mm along the x-axis. The numbers

presented in Table 3 are the results of the comparison of 10 points automatically and evenly selected from the spherical cap surface and with a sphere center shift of 5 mm.

In case of (b), we can observe that our algorithm can accurately measure the radial thickness. The only significant deviations from the real values can be noticed in the points that are on the border line of intersection between the two spheres (e.g., see point 10 in Table 3). These are caused by the segmentation/reconstruction process of the 3D models and not from our radial thickness algorithm. More specifically, the points located exactly at the edge of the reconstructed mesh have real thickness values very close to the segmentation and reconstruction sensitivity/error, which in our case was $1 \times 1 \times 1$ mm as mentioned earlier. Therefore, for these special points, or any other points, with real thickness near to 1 mm or less, the calculated thickness equals to zero.

Results

FE simulation results

The physical model simulations were carried out to investigate the mechanical soft tissue deformation as described in the previous section.

The effective stress distribution in the femoral cartilage for the first scenario with 850N axial compression force is depicted in Fig. 6a. The second simulation scenario (100 N compression force and 45° passive flexion) was divided into 26 smaller steps to capture the different knee movements/rotations. For each simulation step, the stress distribution was measured for each triangle of the cartilage mesh. To calculate the total stress distribution, we added the stress values from each step that corresponded to each and every triangle of the mesh. The result of this procedure is shown in Fig. 6b. For the third and fourth scenario (10° external/internal rotation), the simulation was divided into 11 smaller steps and the total stress was again calculated by adding the stress values of each step, as in the second scenario (see Fig. 6c, d).

Table 2 Calculated knee femoral cartilage thickness in comparison with the real thickness (in mm) using our six sets of test cases (concentric spheres)

Set	Real thickness	Calculated thickness (mm)		
		Min/max	Mean	SD
1	0.5	0.272711/0.883253	0.519278	0.092283
2	1.0	0.939428/1.179634	1.041062	0.048110
3	1.5	1.421366/1.883057	1.558549	0.069742
4	2.0	1.850988/2.095440	2.008072	0.048680
5	2.5	2.353149/2.880350	2.548138	0.070695
6	3.0	2.907595/3.159473	3.022285	0.038382

Table 3 Real thickness versus calculated thickness using 10 point evenly spread along the spherical cap surface)

Point	Real thickness (mm)	Calculated thickness (mm)	Difference
1	3.056090	2.995893	0.060196
2	1.601986	1.426096	0.175890
3	4.142347	4.122402	0.019945
4	4.493361	4.562920	0.069558
5	4.338320	4.422863	0.084543
6	4.100217	4.088711	0.011507
7	4.344876	4.361397	0.016521
8	3.540153	3.603571	0.063418
9	2.350903	2.207294	0.143609
10	1.131383	0.000000	1.131383

Real cap thickness ranges from 0–5 mm (6842 points, mean difference 0.237003 and difference SD 0.278833
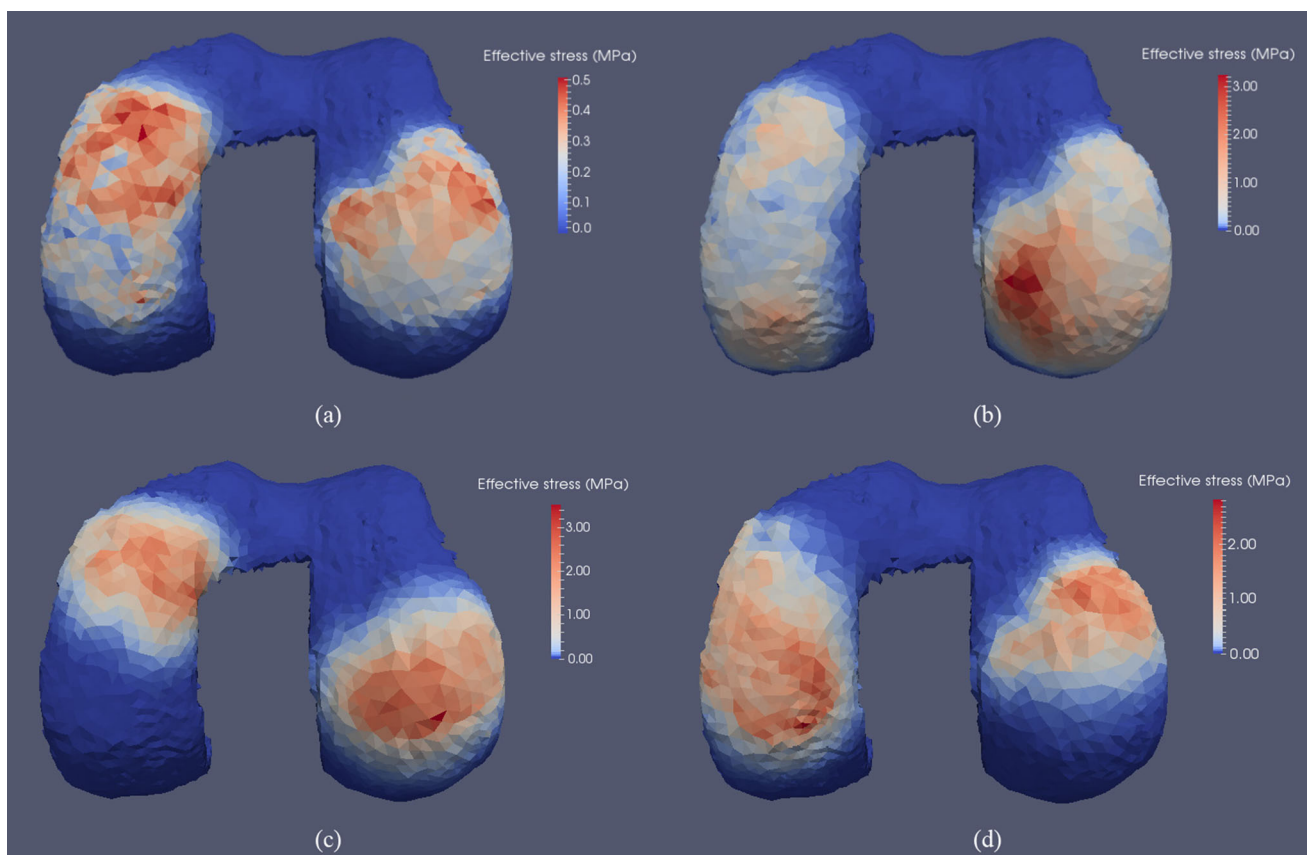
Fig. 6 Effective stress in the femoral cartilage based on our FE simulations: **a** 850 N axial compression force, **b** total stress using 100 N compression force and 45° passive flexion, **c** total stress for 10° of external rotation and **d** total stress for 10° of internal rotation

Overall stress area definition

The overall area of the weight-bearing region was identified by adding the total stress from all four simulation scenarios. All triangle cells with contact pressure exceeding 0.05 MPa were included in the area definition. Pressures below 0.05 MPa were set to 0.0 MPa to filter out insignificantly low values caused by the meshing process. The 0.05 MPa threshold is lower than other similar reported values in the literature [42], and in addition, the detection limit of an ultra-super low-grade pressure indicating film is at most 0.05 MPa and would not register any readings below this threshold. The resulting stress and contact pressure distribution color map are shown in Fig. 7.

Combining the stress values from the first two simulation scenarios, our automatic calculations show that the minimum
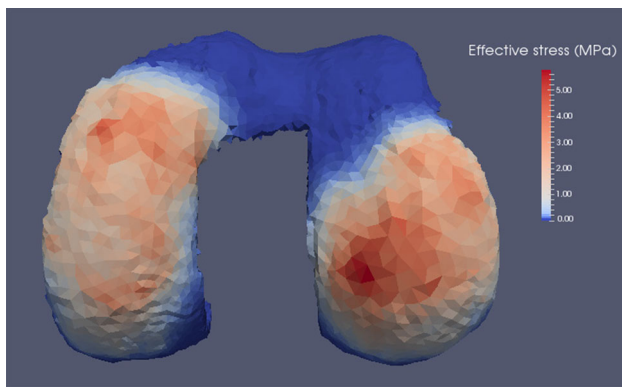
Fig. 7 Overall stress distribution in the femoral cartilage of subject 1 coming from all simulation scenarios

and maximum theta values for the medial condyle of subject 1 (laterality: left) are 218.69° and 279.40°, respectively, i.e., 60.71° angle range. For the lateral condyle, the minimum and maximum theta values are 219.30° and 301.53° respectively, i.e., 82.23° angle range.

When we combine the stress values from all simulation scenarios, including the internal/external knee rotation, our calculations show that the minimum and maximum theta values for the medial condyle of subject 1 are 193.07° and 285.52°, respectively, i.e., 92.45° angle range. For the lateral condyle, the minimum and maximum theta values are 197.95° and 308.57°, respectively, i.e., 110.62° angle range. All angle measurements were based on the direct cylindrical fitting of the femoral cartilage as described in the previous section.

The internal and/or external rotations of the knee significantly influence the shape of the weight-bearing area. According to the above measurements, we can observe that the total length of the stress area increased by 31.73° for the medial condyle and by 28.39° for the lateral condyle of subject 1.

Thickness measurement results

Visual representation of localized femoral cartilage thickness is possible since cartilage thickness measurements were taken at each point in the bone–cartilage interface. The calculated thickness values assigned at each point of the medial and lateral weight bearing areas are displayed as a color map, overlaid on top of the cartilage mesh, with different color variations and intensities.

In order to identify the points of interest where the thickness should be measured and at the same time maintain the shape and size of the weight-bearing region as defined by the overall stress distribution, we divided each condyle area into small stripes using the sagittal plane. For each stripe, we calculated the minimum and maximum theta value, using again our direct cylindrical fitting, and all the points in between these min/max values constitute the set of points for calculating the focal radial thickness. The resulting thickness map for subject 1 is displayed in Fig. 8.

An example of the radial thickness measurements based on our first method of identifying the weight-bearing regions, i.e., fixed regions based on normal gait characteristics, is shown in Fig. 9.

Even a visual comparison of the two different thickness maps of Figs. 8, 9 confirms that the method based on simulation of the cartilage stress areas provides more focused and patient-specific results since it includes subregions that were not considered before.

Developed software application

In order to integrate all the above algorithms, methodologies and features, we implemented a standalone Windows application. The current version can run on Windows XP or above operating systems, and it is written in C++ and utilizes the
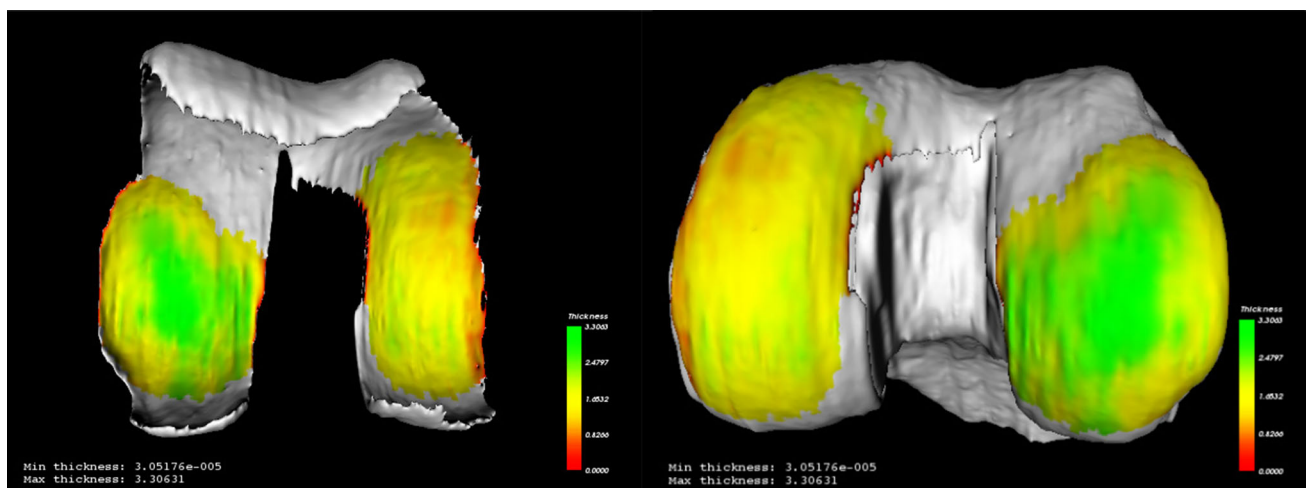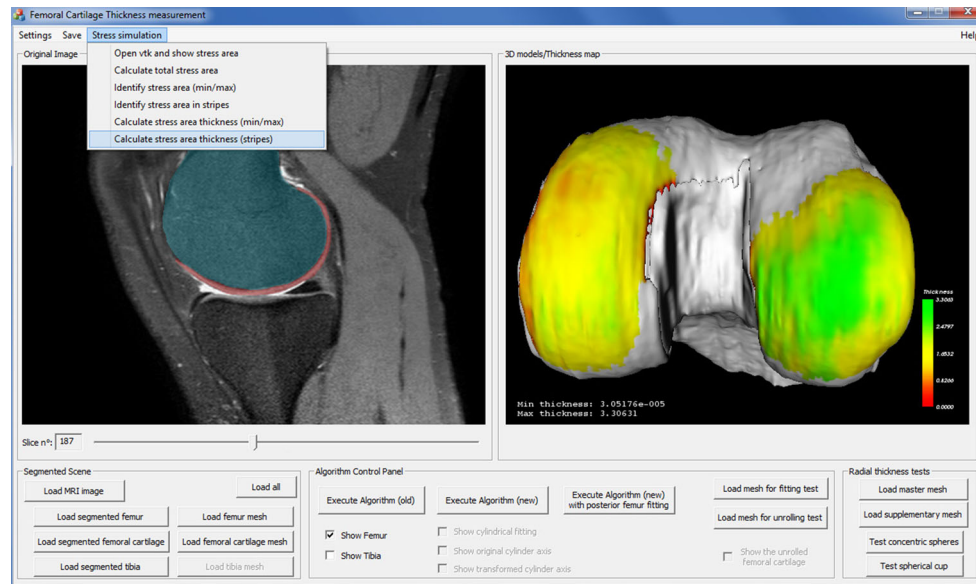

Fig. 8 Focal radial thickness measurements for the femoral cartilage of subject 1, using the overall stress distribution
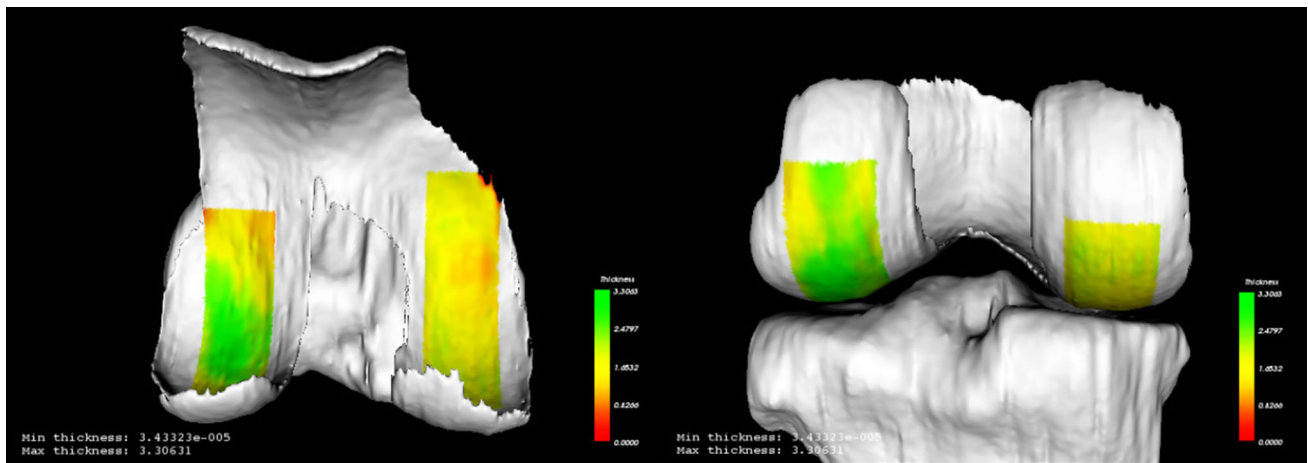
Fig. 9 Localized cartilage thickness using the generic weight-bearing regions based on normal gait characteristics (*green areas* represent thicker cartilage, while *red areas* represent thinner cartilage)

Fig. 10 Developed tool for measuring the focal femoral cartilage thickness near the weight-bearing regions

Insight Segmentation and Registration Toolkit (ITK) and the *Visualization Toolkit* (VTK) open-source libraries. A screenshot of the developed application is shown in Fig. 10.

The application can load a knee MRI in the metaimage format, the segmented knee metaimages (i.e., femur, femoral cartilage and tibia) and the corresponding mesh 3D models (in .vtk format) and automatically calculate the focal femoral cartilage thickness at the weight-bearing regions (over each condyle). The calculated thickness values are then displayed as a color map, overlaid on top of the cartilage mesh. Focusing on the weight-bearing regions, which are usually of the greatest clinical interest, the application could assist and support clinicians in the diagnosis, progression monitoring and treatment of OA.

Discussion

Osteoarthritis (OA) is the most common form of arthritis in the world. The risk of developing musculoskeletal diseases has increased due to obesity, inactivity, lifestyle choices and the aging population. At present, musculoskeletal diseases are the leading cause of disability and productivity loss in Europe and USA [1].

Different morphological, molecular and biochemical biomarkers for predicting or evaluating knee OA have been investigated, including cartilage thickness and volume, as thinning of cartilage is a common manifestation of this pathology. MRI allows the direct visualization, quantification and progression monitoring of cartilage morphology and

is therefore the imaging technique of choice. For that reason, accurate and robust image processing tools are required to perform 3D cartilage analysis.

We have presented a set of techniques to accomplish these goals. An automated method for calculating the focal femoral cartilage thickness was described. Two different ways were used to define the mechanical loading of the knee articulation. The first one was based on generic weight-bearing regions derived from normal gait characteristics and cadaver studies, while the second used a physically based simulation to identify the patient-specific stress distribution of the femoral cartilage, which takes into account the forces and movements of the knee.

Our focal maps originating from the patient-specific simulation data identified more precise weight-bearing areas and stress region boundaries, and revealed subregions that were not considered before. This led to three notable observations. Firstly, the length of the stress area of the medial condyle is longer than the one from the lateral condyle. This is also verified by the already known movement/rotation of the medial condyle. The contact area is bigger because it follows the shape of the menisci and the fact that the lateral meniscus has a larger "C" size. The second observation is that the width of both regions of interest (weight-bearing areas), especially on the lateral condyle, is larger. It covers almost the whole width of the condyle area and with considerably higher stress values near the "inside" edge (toward the medial side) of the lateral condyle. This region was not previously included by our first method that used the generic definition of the weight-bearing areas based on normal gait characteristics. The third observation has to do with the effect of the internal/external rotation of the knee to the contour/outline of the weight-bearing areas. Our simulation results confirmed that the contribution to these rotations significantly alter the overall stress distribution since new contact points were revealed.

Even if we could achieve a more precise analysis, changes in cartilage thickness are still highly variable, and more sensitive measurements cannot compensate entirely for patient heterogeneity with respect to cartilage loss. Using patient-specific data gives a considerable advantage when dealing with stress-related OA assessments. Our approach takes into account these subject-specific characteristics and knee morphology instead of generic striped central regions. Undoubtedly, a large part of the area overlaps with the generic central femoral regions defined in the nomenclature article by Eckstein et al. [43] and subsequent follow-up studies [44].

Further testing and validation of our methods are needed since we only used a small number of healthy subjects in our study. As future work, we plan to validate the reproducibility of our work using a larger sample of subjects. This larger dataset should include pathological patients, with different stages of medial and lateral OA, as well as subjects with varus/valgus malalignment which can increase the tibiofemoral load, but without established OA. Future studies will also incorporate the cruciate and collateral knee ligaments in the FE model. In addition, we are considering creating a representative stress distribution model from a large statistical sample size of subjects, in order to provide a rapid and fully automatic way of identifying the weight-bearing areas of the femoral cartilage.

A possible limitation and bottleneck in our methods is the increased segmentation time due to the manual correction step introduced in the semiautomatic segmentation. Having T1 images, instead of T2, would increase the accuracy of our level-set algorithm and would decrease the required manual corrections, therefore reducing the overall segmentation time. The Osteoarthritis Initiative (OAI) [45] is a rich source of open access MR sequences used for numerous OA studies during the last few years. We intend to utilize these OAI resources for validating our methods and further study the focal cartilage thickness.

Computer-assisted methods are major research subjects in medical informatics and diagnostic radiology. CAD is a well-established concept [46], and physicians use computer outputs in a complementary way to support their final diagnosis, for knee surgery planning, prosthesis design, etc. The need to improve the quality of health care has led to a strong demand for CAD systems that can provide accurate, repeatable and objective feature measurements.

To the best of our knowledge, 3D FE simulations with subject-specific models have never been used before to define and calculate the femoral cartilage weight-bearing areas and the focal cartilage thickness. Our work can support clinicians during the diagnosis, treatment and follow-up of knee osteoarthritis and moves a step closer toward personalized medicine, a customizable model of healthcare with medical decisions and practices tailored to the individual patient.

Compliance with Ethical Standards

Conflicts of interest Marios Pitikakis, Andra Chincisan, Nadia Magnenat-Thalmann, Lorenzo Cesario, Patrizia Parascandolo, Loris Vosilla and Gianni Viano declare that they have no conflict of interest related to the study described in the article.

Statement of informed consent Informed consent was obtained from all volunteer subjects for being included in the study.

References

1. European Musculoskeletal Conditions Surveillance and Information Network (2012) Musculoskeletal health in Europe: Report v5.0. http://www.eumusc.net Accessed 17 December 2014

2. Eckstein F, Maschek S, Wirth W, Hudelmaier M, Hitzl W, Wyman B, Nevitt M, Hellio Le Graverand MP (2008) One year change of knee cartilage morphology in the first release of participants from the Osteoarthritis Initiative Progression Subcohort: association with sex, body mass index, symptoms, and radiographic OA status. Ann Rheum Dis 68:674–679

3. Eckstein F, Cicuttini F, Raynauld J, Waterton JC, Peterfy C (2006) Magnetic resonance imaging (MRI) of articular cartilage in knee osteoarthritis (OA): morphological assessment. Osteoarthr Cartil 14(Suppl A):46–75

4. Raynauld JP, Kauffmann C, Beaudoin G, Berthiaume MJ et al (2003) Reliability of a quantification imaging system using magnetic resonance images to measure cartilage thickness and volume in human normal and osteoarthritic knees. Osteoarthr Cartil 11:351–360

5. Glaser C, Draeger M, Eckstein F, Englmeier KH, Reiser M (2002) Cartilage loss over two years in femoro-tibial osteoarthritis. Radiology 225(Suppl):330

6. Koo S, Gold GE, Andriacchi TP (2005) Considerations in measuring cartilage thickness using MRI: factors influencing reproducibility and accuracy. Osteoarthr Cartil 13:782–789

7. Amin S, LaValley MP, Guermazi A, Grigoryan M, Hunter DJ, Clancy M, Niu J, Gale DR, Felson DT (2005) The relationship between cartilage loss on magnetic resonance imaging and radiographic progression in men and women with knee osteoarthritis. Arthritis Rheum 52:3152–3159

8. Raynauld JP, Martel-Pelletier J, Berthiaume MJ, Beaudoin G et al (2006) Long term evaluation of disease progression through the quantitative magnetic resonance imaging of symptomatic knee osteoarthritis patients: correlation with clinical symptoms and radiographic changes. Arthritis Res Ther 8:R21

9. Pelletier JP, Raynauld JP, Berthiaume MJ, Abram F, Choquette D et al (2007) Risk factors associated with the loss of cartilage volume on weight-bearing areas in knee osteoarthritis patients assessed by quantitative magnetic resonance imaging: a longitudinal study. Arthritis Res Ther 9:R74

10. Williams TG, Holmes A, Waterton J, Maciewicz R, Nash A, Taylor C (2006) Regional quantitative analysis of knee cartilage in a population study using MRI and model based correspondences. In: IEEE international symposium on biomedical imaging, Arlington, VA

11. Williams TG, Holmes AP, Bowes M, Vincent G, Hutchinson CE et al (2010) Measurement and visualisation of focal cartilage thickness change by MRI in a study of knee osteoarthritis using a novel image analysis tool. Br J Radiol 83:940–948

12. Wirth W, Le Graverand M-PH, Wyman BT, Maschek S, Hudelmaier M et al (2009) Regional analysis of femorotibial cartilage loss in a subsample from the osteoarthritis initiative progression subcohort. Osteoarthr Cartil Osteoarthr Res Soc 17(3):291–297

13. Tamez-Peña JG, Barbu-McInnis M, Totterman S (2006) Unsupervised definition of the tibia-femoral joint regions of the human knee and its applications to cartilage analysis. In: Proceedings of SPIE 6144, medical imaging 2006: image processing, 61444K

14. Duryea J, Iranpour-Boroujeni T, Collins JE et al (2014) Local-area cartilage segmentation (LACS): a semi-automated novel method of measuring cartilage loss in knee osteoarthritis. Arthritis Care Res (Hoboken) 66(10):1560–1565

15. Bae JY, Park KS, Seon JK et al (2012) Biomechanical analysis of the effects of medial meniscectomy on degenerative osteoarthritis. Med Biol Eng Comput 50(1):53–60

16. Mononen ME, Julkunen P, Töyräs J et al (2011) Alterations in structure and properties of collagen network of osteoarthritic and repaired cartilage modify knee joint stresses. Biomech Model Mechanobiol 10(3):357–369

17. Pena E, Calvo B, Martinez MA, Doblare M (2006) A three-dimensional finite element analysis of the combined behavior of ligaments and menisci in the healthy human knee joint. J Biomech 39(9):1686–1701

18. Dong Y, Hu G, Dong Y, Hu Y, Xu Q (2012) The effect of meniscal tears and resultant partial meniscectomies on the knee contact stresses: a finite element analysis. Computer methods in biomechanics and biomedical engineering, pp 1-12

19. RheumaSCORE (2014) http://www.research.softeco.it/rheumascore.aspx Accessed 17 December 2014

20. Parascandolo P, Cesario L, Vosilla L, Viano G (2014) Computer aided diagnosis: state-of-the-art and application to musculoskeletal diseases. In: Magnenat-Thalmann N, Ratib O, Choi HF (ed) 3D multiscale physiological human. Springer, pp 277–296. http://www.springer.com/us/book/9781447162742

21. Softeco Sismat Srl (2014) http://www.softeco.it. Accessed 17 Dec 2014

22. Barbieri F, Parascandolo P, Vosilla L, Cesario L, Viano G, Cimmino MA (2012) Assessing MRI erosions in the rheumatoid wrist: a comparison between RAMRIS and a semi-automated segmentation software. Ann Rheum Dis 71((Suppl3)):709

23. Catalano CE, Robbiano F, Parascandolo P, Cesario L, Vosilla L, Barbieri F, Spagnuolo M, Viano G, Cimmino MA (2013) Exploiting 3D part-based analysis, description and indexing to support medical applications. Med Content Based Retr Clin Decis Support LNCS 7723:21–32

24. Parascandolo P, Cesario L, Vosilla L, Pitikakis M and Viano G (2013) Smart Brush: A real time segmentation tool for 3D medical images. In: IEEE, Image and signal processing and analysis (ISPA), 2013 8th international symposium, pp 689–694

25. Fedkiw R, Osher S (2002) Level set methods and dynamic implicit surfaces. Springer, Berlin

26. Bhaidasna Z, Mehta S (2013) A review on level set method for image segmentation. Int J Comput Appl 63(11):20–22

27. Lorensen WE, Cline HE (1987) Marching cubes: a high resolution 3D surface construction algorithm. In: Proceedings of ACM SIGGRAPH, pp 163–169

28. Kauffmann C, Gravel P, Godbout B, Gravel A et al (2003) Computer-aided method for quantification of cartilage thickness and volume changes using MRI: validation study using a synthetic model. IEEE Trans Biomed Eng 50(8):978–988

29. Chernov N, Ma H (2011) Least squares fitting of quadratic curves and surfaces. In: Yoshida SR (ed) Computer Vision. Nova Science Publishers, pp 285–302. https://www.novapublishers.com/catalog/product_info.php?

30. Lukács G, Martin R, Marshall D (1998) Faithful least-squares fitting of spheres, cylinders, cones and tori for reliable segmentation. ECCV 1998:671–686

31. Andrews J, Sequin CH (2013) Type-constrained direct fitting of quadric surfaces. Comput Aided Des Appl 11(1):107–119

32. Anderson E, Bai Z, Bischof C, Blackford S et al (1999) LAPACK users' guide. Society for Industrial and Applied Mathematics. doi:10.1137/1.9780898719604

33. Taubin G (1991) Estimation of planar curves, surfaces and nonplanar space curves defined by implicit equations, with applications to edge and range image segmentation. IEEE Trans Pattern Anal Mach Intell 13:1115–1138. doi:10.1109/34.103273

34. Alliez P, Rineau L, Tayeb S, Tournois J, Yvinec M (2014) 3D mesh generation. In: CGAL user and reference manual. CGAL Editorial Board, 4.5 edn https://www.cgal.org Accessed 17 Dec 2014

35. Sibole S, et al (2010) Open knee: a 3D finite element representation of the knee joint. In: 34th annual meeting of the American Society of Biomechanics

36. Maas SA, Ellis BJ, Ateshian GA et al (2012) FEBio: finite elements for biomechanics. J Biomech Eng 134(1):011005
37. Hemmerich A, Brown H, Smith S et al (2006) Hip, knee, and ankle kinematics of high range of motion activities of daily living. J Orthop Res 24(4):770–781
38. Kutzner I, Heinlein B, Graichen F et al (2010) Loading of the knee joint during activities of daily living measured in vivo in five subjects. J Biomech 43(11):2164–2173
39. Wang D, Shi L, Heng PA (2007) Radial thickness calculation and visualization for volumetric layers. In: The Insight Journal—2007 MICCAI open science workshop. http://hdl.handle.net/1926/552. Accessed 17 Dec 2014
40. Moller T, Trumbore B (1997) Fast, minimum storage ray/triangle intersection. J Graphics Tools 2(1):21–28
41. Shepherd DE, Seedhom BB (1999) Thickness of human articular cartilage in joints of the lower limb. Ann Rheum Dis 58(1):27–34
42. Oshkour AA, Osman NAAbu, Davoodi MM et al (2011) Knee joint stress analysis in standing. In: 5th Kuala Lumpur international conference on biomedical engineering. IFMBE Proceedings 35:179–181
43. Eckstein F, Ateshian G, Burgkart R et al (2006) Proposal for a nomenclature for magnetic resonance imaging based measures of articular cartilage in osteoarthritis. Osteoarthr Cartil 14(10):974–983
44. Cotofana S, Buck R, Wirth W, Roemer F, Duryea J, Nevitt M, Eckstein F (2010) Cartilage thickening in early radiographic knee osteoarthritis: a within-person, between-knee comparison. Arthritis Care Res (Hoboken) 64(11):1681–90
45. The Osteoarthritis Initiative (2014) www.oai.ucsf.edu. Accessed 28 May 2015
46. Doi K (2007) Computer-aided diagnosis in medical imaging: historical review, current status and future potential. Comput Med Imaging Graph 31:198–211